Comparative Analysis of Coupled and Uncoupled 3D Finite Elements Models for Masonry Structures Subjected to Settlements

Prosperi, Alfonso; Longo, Michele; Korswagen, Paul A.; Korff, Mandy; Rots, Jan G.

Comparative Analysis of Coupled and Uncoupled 3D Finite Elements Models for Masonry Structures Subjected to Settlements

Alfonso Prosperi[1]([✉]) [iD], Michele Longo[1] [iD], Paul A. Korswagen[1] [iD], Mandy Korff[1,2] [iD], and Jan G. Rots[1]

[1] Faculty of Civil Engineering and Geosciences, Delft University of Technology, Stevinweg 1, 2628 Delft, The Netherlands
a.prosperi@tudelft.nl
[2] Deltares, P.O BOX, 177, 2600 MH Delft, The Netherlands

Abstract. In the Netherlands, subsidence due to different causes is linked to damage to the ubiquitous masonry structures. Finite element (FE) analyses can be used to assess the response of the structures subjected to settlements. This paper presents the comparison between three-dimensional FE modelling strategies to investigate the response of an unreinforced masonry building on a strip foundation. The aim is to investigate whether different modelling approaches demonstrate consistent results. The soil-structure system is modelled employing two strategies: a coupled model, in which the structure is tied to the soil volume, and an uncoupled approach that divides the soil and structure into two sub-systems. Two displacement fields, imposed at the bottom of the soil volume, idealize various shapes of the subsidence troughs, with increasing intensity measured by their distortion. Non-linear interfaces are used to simulate the soil-foundation interaction, and their stiffness values vary based on the type of model. The displacements, interface stresses and crack patterns of the selected modelling strategies are consistent. The interface types do not influence the response of the façade, whereas the shape of the settlement does play a key role. The uncoupled models exhibit, on average, slightly higher values of damage than coupled models for a given imposed distortion. The two modelling strategies require almost the same computational time and show similar convergence. Because of the limited contribution of small soil volumes in uncoupled models, the superstructure sub-system can be directly utilized to assess the response of structures undergoing vertical displacements, thereby reducing the modelling burden.

Keywords: Masonry · Damage · Settlements · Numerical models

1 Introduction

Masonry buildings are prevalent throughout the Netherlands even in places with compressible peat and clay strata, namely "soft soils". Although some buildings rely on piled foundations, which reach deep and stable soil layers, many buildings still were built on shallow foundation systems (i.e. rafts, strips) and are since then directly exposed to ground movements.

Land subsidence, due to a complex combination of drivers, causes the progressive occurrence of uneven settlements that manifest as cracks and deformations in the buildings.

Current predictions that include the effect of climate change for 2050 (Fig. 1a) show that the densely populated western part of the Netherlands is expected to exhibit high rates of land subsidence. Thus, many old masonry buildings that rest on unreinforced masonry strip foundations (Fig. 1b) could experience differential settlements that pose a risk for damage.

(a) - Cumulative subsidence prediction (2020-2050)

(b) - Risk of differential settlements for buildings on shallow foundations

Neglegible (<3cm) Limited (3–10cm) Moderate (10–20cm) Consistent (20–40cm) High (40-60cm) Very High (>60cm)

Very small small moderate high Very high
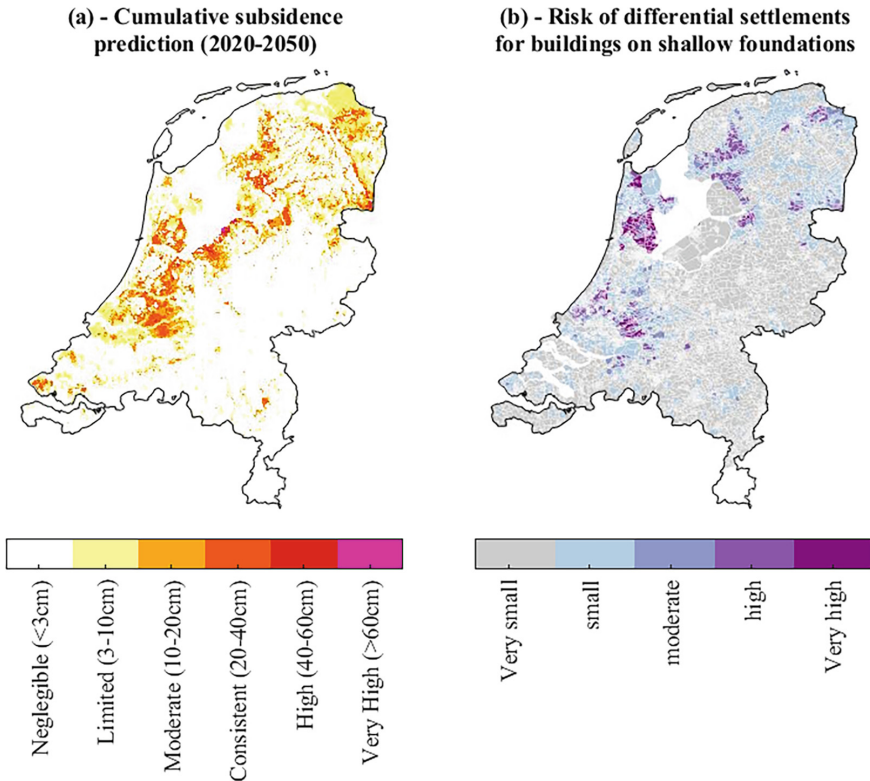
Fig. 1. (a) Cumulative subsidence prediction map for the period 2020–2050, including the effect of climate change and (b) Risk of differential settlements for buildings on shallow foundations. Data retrieved from klimaateffectatlas.nl [1, 2].

In this context, predictions are needed to evaluate the response of the exposed masonry structures and, in turn, to identify areas in which buildings could be highly vulnerable.

Numerical simulations provide a valuable tool to investigate the structural behaviour of specific building typologies, whereas empirical observations may be limited to a few cases or unavailable.

Recent studies (e.g. [3–6]) focus on modelling structures undergoing subsidence-related settlements and explore the effect of different structural features on the response of the buildings. Although the availability of computational resources increased in the last decades, numerical simulations can still have a high modelling burden and computational cost due to complex meshes and the high number of elements, and could even run for days in terms of CPU time [4]. Consequently, refined approaches are essential to limit computational costs and diminish the modelling workload, with a focus on the numerous analyses required to evaluate the structural response in a probabilistic framework.

This study presents the comparison between two modelling approaches herein adopted to evaluate the response of masonry structures on strip foundations undergoing settlements.

The difference between the adopted modelling approaches lies in the way the soil-structure interaction is modelled, which is detailed in the next sections. The results of the two models are compared to investigate their differences.

This paper begins with Sect. 2, in which the workflow of this study is presented. In Sect. 3, the selected modelling approaches are detailed. In Sect. 4, the results are presented, whereas they are discussed in Sect. 5. Section 6 gathers the main conclusions.

2 Methodology

In this study, two 3D modelling approaches for masonry structures subjected to settlements are selected from the state-of-the-art and used to simulate the response of a study case, already adopted in previous research, i.e., [4–6].

The models include the influence of a soil volume that is used to represent the soil-structure interaction. A sensitivity analysis is carried out by fictitiously increasing the thickness of the soil stratum to further investigate its role.

Moreover, additional sensitivity analyses investigate the influence of the mesh size of the numerical model on the results.

The results of the two modelling approaches are compared in terms of displacements, stresses and damage. The differences and similarities between the two modelling approaches are thus evaluated.

3 Finite Element Models

In this study, two 3D modelling approaches inspired by the state-of-the-art are selected and used for the analysis of a masonry structure subjected to subsidence-related settlements. Two different displacement fields are imposed in the model to idealize the effect of the subsidence processes, as further described in the following sub-sections.

Figure 2 illustrates the two selected models built with the finite element software Diana FEA 10.7:

- The **coupled** model (Fig. 2a), a shell-elements three-dimensional model of the building and strip foundation, without floors and party walls, similar to [4, 7–10]; The model includes the effect of the material non-linearities. Moreover, inspired by the

work of [11], the model includes a dummy linear-elastic soil layer, tied to the structural model using contact interface elements; The dummy soil does not simulate the accurate response of the soil stratum but facilitates the representation of soil-structure interaction. The displacement field is applied at the bottom of the soil volume.

- The **uncoupled** model (Fig. 2b), is made by two sub-systems that separate the soil and the superstructure. Figure 2b0 shows the soil sub-system; The input displacement field is applied at the bottom of this soil model, while the displacement obtained on its top surface, namely the free-field displacements (i.e., the displacement obtained in the absence of the buildings), are used as an input in the structural model Fig. 2b1. The soil sub-system is included for a consistent comparison with the results of the coupled approach, as it was initially hypothesized that the soil volume could slightly decrease the distortion of the applied displacement fields that are transmitted to the superstructure. The structure model Fig. 2b1 is described by the same feature of the structural portion of the coupled approach (Fig. 2a). The main difference consists in the type of interface, i.e., boundary interface, which represents the role and the interaction with the untied soil volume. The displacements obtained from the top edge of the soil subsystem (Fig. 2b0) are applied at the bottom of the boundary interface in the superstructure subsystem.

Therefore, both modelling approaches differ in the way the interaction with a soil stratum beneath the foundation and the response of the superstructure are schematized.

3.1 Geometry and FEM Discretization

Superstructure

The selected case study corresponds to a two-storey masonry building. The façade of the building has a width of 8 m, and a total height of 7 m and it represents a single-wythe wall [5] (0.1 m). The lateral walls in the models have the same height as the façade and half of its length; This is because the models make use of the structural symmetry and only depict half of the building.

The models include the masonry strip foundation system below the walls, commonly observed in such old buildings, with a base "B" (perpendicularly to the façade) of 500 and a height of 600 mm. The models include openings underneath masonry lintels. The lintels, the strip foundation and the walls are discretized with quadrilateral (8 nodes) and triangular (6 nodes) shell elements, with an average mesh size of 200×200 mm. A 3×3 Gauss integration scheme is employed in the plane of the elements while 5 integration points following the Simpson rule are used in the thickness of the shell elements.

The superstructure represents old masonry buildings with timber roofs and timber floors; These elements, however, were not included in the models, as they were observed to not influence significantly the response of this structure when subjected to settlement [4].

Soil volume

The soil volume adopted in the analyses was assumed to have a height "H" equal to 600 mm, corresponding to 1.2 times "B" (the base of the foundation). The value of 600 mm corresponds to an initial guess, obtained considering the depth of the pressure

(a) Coupled approach:

(b) Uncoupled approach:
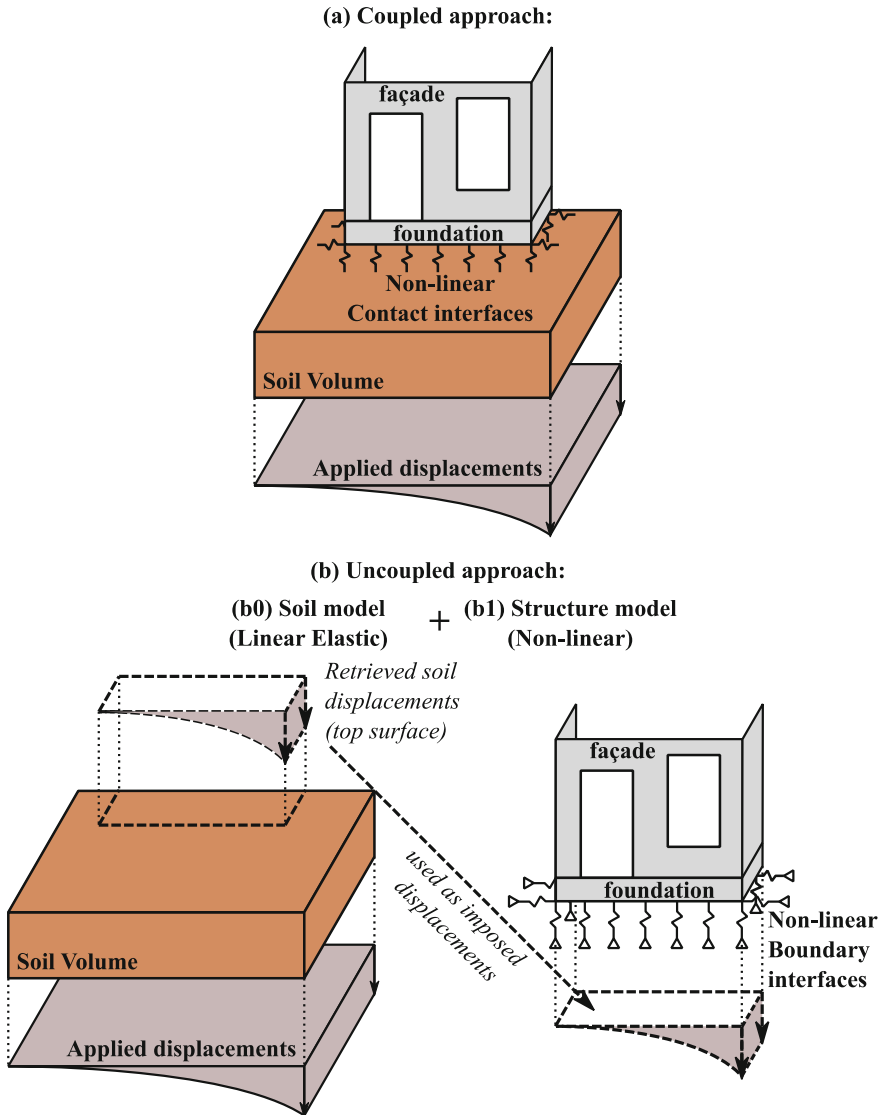
Fig. 2. The adopted modelling approaches: (a) the coupled model consisting of a soil volume to which the displacement field is imposed linked to the structure via non-linear contact interfaces and (b) uncoupled approach, that includes (b1) the soil model, to which the displacement field is imposed and (b2) the structural model.

bulbs for the strip foundation [12] based on the solution of the Boussinesq equation. In particular, the depth of the pressure bulb that corresponds to 50% of the applied superficial load is considered, i.e. approximately equal to 1.2 B. The soil height H is hypothesized to influence the results; Thus, two additional soil heights are considered

to further evaluate their influence. The additional soil heights are equal to 2 and 4 times the initial guess, i.e., 1200 and 2400 mm respectively.

The borders of the soil volume are placed at a distance of 8 m from the walls; Thus, the soil is represented by a 24 m × 12 m × "H" volume discretized by brick (20 nodes) and wedge (15 nodes) elements. The mesh size of the soil block close to the building (elements within 2 m from the building) ranges from 200 to 400 mm while ranges from 400 to 800 mm for the rest of the soil elements. Gauss integration 2 × 2 × 2 is selected for the soil volume.

3.2   Material Properties

The non-linear cracking behaviour of the masonry material was modelled employing an orthotropic, smeared crack/shear/crush constitutive law, i.e., the Engineering Masonry Model [13, 14]. The material properties of the selected fired clay brick masonry (Table 1) are retrieved from the literature and the Dutch norm [14–16] and were applied to the walls, lintels and strip foundation. Additionally, the crack bandwidth is determined using Govindjee's [17] projection method.

Table 1. Material properties adopted in the FE models.

Material properties	Symbol	Unit of measure	Value
Young's modulus vertical direction	E_y	[MPa]	5000
Young's modulus horizontal direction	E_x	[MPa]	2500
Shear modulus	G_{xy}	[MPa]	2000
Bed joint tensile strength	f_{ty}	[MPa]	0.10
Minimum head-joint strength	$f_{tx,min}$	[MPa]	0.15
Fracture energy in tension	$G_{ft,I}$	[N/mm]	0.01
Angle between stepped crack and bed-joint	α	[rad]	0.50
Compressive strength	f_c	[MPa]	8.50
Fracture energy in compression	G_c	[N/mm]	20.00
Friction angle	φ	[rad]	0.70
Cohesion	c	[MPa]	0.15
Fracture energy in shear	G_s	[N/mm]	0.10
Mass density	ρ	[Kg/m^3]	1708

The properties of the selected soil are characterized by Young's modulus E equal to 29, the shear modulus G equal to 10 MPa and the Poisson's ratio υ equal to 0.45.

Moreover, the selected soil is characterized by a friction angle of 0.29 rad (or about 17°) and no cohesion. Moreover, a mass of 2000 kg/m^3 and a K_0 of 0.5 are assigned to the soil block.

3.3 Soil-Foundation Interaction

Both modelling approaches use non-linear interfaces to represent the soil-foundation interaction. The models make use of the Coulomb-friction constitutive law, with no tensile strength and characterized by the properties of the selected soil.

In the case of the coupled models, the superstructure is coupled with the soil volume, while in the uncoupled approach, the two subsystems are divided. In the first modelling approach, interface elements should be able to transmit stresses and displacement directly to the superstructure, whereas in the latter the interface should also represent the behavior, in terms of stiffness, of the missing soil volume. Therefore, in the following subsections, two different approaches are reported to compute the stiffness of the different types of interfaces.

Table 2. Values of the vertical and tangential interface stiffness of the adopted models (for a mesh size of 200×200 mm).

Interface type	Parameter	Value	Unit of measurement
Contact	K_n	2.22E–01	N/mm^3
	K_t	2.02E–02	
Boundary	K_n	3.35E–02	
	K_n (foundation edges)	4.10E–02	
	K_t	2.26E–02	

Contact Interfaces

The contact interface normal and tangential stiffnesses are computed using the equations reported by [18]:

$$K_n = \left(\frac{2}{3}\right)^2 \frac{E}{2(1+\upsilon)\frac{l_{interface}}{10}} \tag{1}$$

$$K_t = \frac{K_n}{11} \tag{2}$$

where E is the Young's modulus of the adjacent soil and υ the Poisson's ratio; $l_{interface}$ is the length of the single interface element, and depends thus on the mesh size [18]. The division of $l_{interface}$ by 10 comes from the hyphotesis that the virtual thickness of the interface is equal to 0.1 times the length of the element. The computed values are reported in Table 2.

Boundary Interfaces

The boundary interface normal and tangential stiffnesses are computed using the equations reported by [19] and proposed by [20, 21], for arbitrarily shaped foundations on a

homogeneous half-space [22]:

$$K_n = \frac{GL}{1 - \upsilon}\left[0.73 + 1.54\left(\frac{B}{L}\right)^{0.75}\right] \tag{3}$$

$$K_t = GL\left[\frac{1}{2 - \upsilon}\left[2 + 2.5\left(\frac{B}{L}\right)^{0.85}\right] - \frac{0.2}{2(0.75 - \upsilon)}\left[1 - \frac{B}{L}\right]\right] \tag{4}$$

where K_n, and K_t in Eqs. (3) and (4) represent the static stiffnesses for a rigid foundation respectively for the normal, and tangential (i.e. in the plane of the façade) directions to the soil surface. G is the soil shear modulus, B represents the foundation base (i.e., perpendicularly to the façade), while L is the foundation length (equal to the length of the façade). The vertical soil stiffness is not uniform, and should increase near the edges of the foundation [19]; It is possible to consider this effect enhancing the values of the vertical stiffness K_n by a coefficient k_z computed as:

$$k_z = \frac{K_n}{BL} \tag{5}$$

The values of K_n multiplied by k_z applied at both sides of the façade for a length equal to 1/6 of its total length. The values of K_n, and K_t are then divided by B and L to obtain smeared values of the normal and shear linear stiffness. The computed values are reported in Table 2.

3.4 Boundary Restrains

In both modelling approaches, half of the building is modelled. Symmetric boundary conditions are applied to the edges of the transversal walls and transversal strip foundations. In-plane translation and rotation about the vertical axis are constrained at these locations. Vertical and horizontal translational supports are applied to the bottom side of the boundary interface of the uncoupled model. For the soil volume, translational supports in the out-of-plane directions are employed. The supports at the lateral side of the soil block are removed during the application of the settlement action to allow for the curvature of the soil block.

3.5 Loading

Two settlement shapes, conformed to a Gaussian curve and based on literature data [23–25], fictitiously simulate the reduction of support due to the settlements without having the soil unrealistically pull on the foundations [5].

Therefore, the imposed settlements are not the result of a specific driver within the soil, but represent an idealization. The settlement shapes are imposed at the bottom of the soil volume as input displacements and are computed using Eq. (6):

$$S(x) = S_{max}\left\{(-1)^{\iota}\left(e^{\left[\frac{-(x-D_x)^2}{2x_i^2}\right]}\right)\right\} \tag{6}$$

where x is the horizontal distance between the left and right sides of the building's façade, D_x is the horizontal distance between the symmetry axis of the Gaussian curve and the one of the building's façade, and x_i is the distance from the symmetry axis of the curve to the point of inflection. The term "ι" enables controlling the convexity of the Gaussian curve. The two settlement shapes are obtained by arbitrarily imposing the parameters D_x and x_i equal to 1.0 * L and 0.25 * L respectively, and ι equal to 1 in the case labelled as "hogging" (Fig. 3a) and 0 for "sagging" (Fig. 3b). Moreover, the amplitude of the settlement shapes, i.e., the maximum settlement, is set via the scalar S_{max} to ensure that the angular distortion imposed at the bottom of the soil volume, in the area beneath the building (Fig. 3) is equal to 1/300. In particular, the imposed angular distortion corresponds to the maximum value along the area beneath the façade. To further clarify, the two settlement shapes imposed at the base of the soil volume represent the outcome of subsidence processes which occur in the soil strata deeper than the one included in the models.
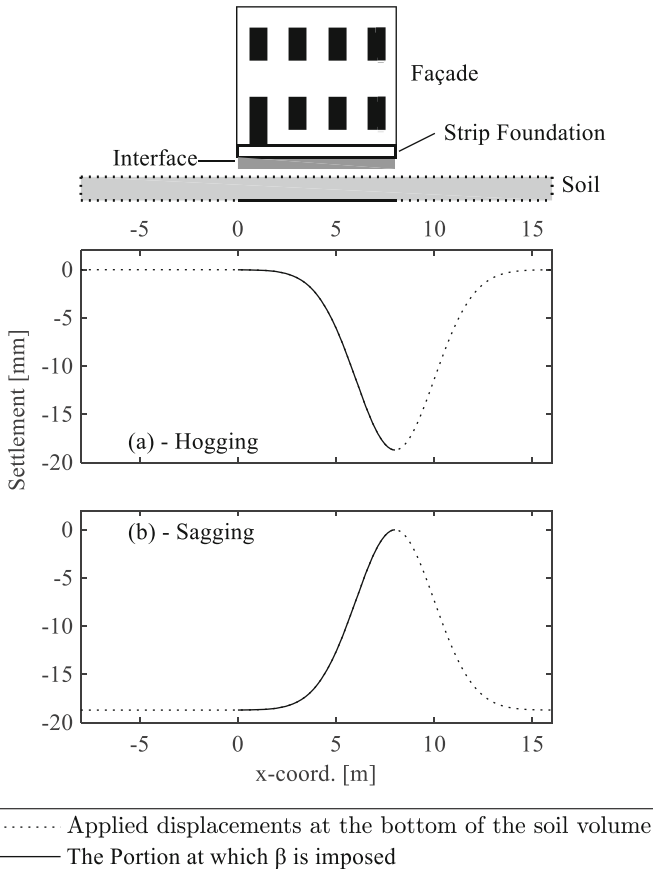

Fig. 3. Settlement profiles applied in the finite element models: (a) Hogging and (b) Sagging.

A three-phased load application procedure is adopted for the coupled model models: first, the K_0 procedure is analyzed for the soil block only. Then, the building is added and the self-weight of the structure is applied in a single step to compute the initial stress state, and then the settlement deformation is applied in 374 steps (with a load rate of 0.05 mm/step). In the uncoupled model, the first phase is conducted as a separate analysis, while the same settings are kept for the gravity and settlement load. The secant (quasi-Newton) method is employed as the iterative method. Both force and displacement norms must be satisfied simultaneously to achieve convergence. The line-search option for the iteration method is activated, which is an option that stabilizes the convergence behaviour and aids the convergence speed [18]. The maximum number of iterations per step is equal to 75.

3.6 Damage Assessment

The outputs of the numerical models are used to quantify the damage progression and accumulation using the parameter Ψ, [26], based on the number of cracks, their length and opening. The corresponding damage severity is then categorized according to the system proposed by [27], shown in Table 3.

Table 3. Damage scale with the classification of visible damage and the corresponding discretization of the damage parameter in sub-levels (from [26, 28, 29]).

Damage level	Degree of damage	Approximate crack width	Parameter of damage
DL0	No damage	Imperceptible cracks	$\Psi < 1$
DL1	Negligible	up to 0.1 mm	$1 \leq \Psi < 1.5$
DL2	Very slight	up to 1 mm	$1.5 \leq \Psi < 2.5$
DL3	Slight	up to 5 mm	$2.5 \leq \Psi < 3.5$
DL4	Moderate	5 to 15 mm	$\Psi \geq 3.5$

It should be noted that the parameter Ψ was originally proposed to study the initiation and propagation of light damage, i.e. cracking associated with crack width up to 5 mm (DL3 in Table 3). Therefore, this study focuses on this specific type of damage in masonry structures subjected to settlements. Damage higher than that could result in cracking associated with a significant reduction of the structural capacity, which could be better measured with different metrics.

4 Results

4.1 Displacements

In this study, a distinction is made between the displacements obtained in the numerical analyses:

- the input displacements (applied at the bottom of the soil block);
- the displacements obtained at the bottom of the interface elements, i.e., the top edge of the soil block;
- the displacements at the bottom of the façade, i.e., the top edge of the strip foundation.

In each step of the numerical analyses, it is possible to evaluate the results at specific values of (angular) distortion. Figure 4 shows the displacements obtained from the two modelling approaches for an imposed angular distortion of 1.00‰ (or 1/1000) for different soil heights. For the uncoupled models with a soil height smaller or equal to 1200 mm (Fig. 4b, d), the elastic soil block does not significantly reduce the displacements imposed at its bottom due to its limited height, and thus its contribution can be considered negligible. This is not the case for the uncoupled modes, in which the input displacements and the one retrieved at the bottom of the interface are observed to differ. Regarding the coupled model (Fig. 4a–e), the displacements obtained at the bottom of the interface are observed to be almost identical to the ones of the façade for all the considered soil heights, as they are influenced by the superstructure tied to the soil block. For both the coupled and uncoupled models, the analyses clearly show how the stiffness of the superstructure flattens down the effect of the imposed displacements.

From the displacements at the bottom of the soil block, interfaces and façade, the angular distortion can be computed. The values of the angular distortion correspond to the maximum values along the considered level, i.e., soil beneath the building, interface or façade. Figure 5 illustrates the relationship between the different angular distortion values for all the steps of the numerical analyses. In other words, it provides an overview of how the input distortion, i.e., soil β, gets transmitted to the interface, i.e., interface β and then to the façade, i.e., façade β. As previously observed in Fig. 4, the distortion imposed at the base of the soil volume does not differ from the one that reaches the bottom of the interface for models uncoupled with a soil height lower or equal to 1200 mm for both hogging and sagging (Fig. 4a, b, respectively). Moreover, the difference between the results of the coupled and uncoupled models in Fig. 4a, b originated from the presence of the superstructure directly tied to the soil system. In other words, the weight and stiffness of the structure modify the displacements at the top level of the soil volume that would be otherwise equal to the one applied at the bottom in the absence of the structure (free-field displacement). For instance, for the models with a soil height of 600mm and a soil β equal to 1.00‰ (or 1/1000) in hogging, the coupled model exhibits an interface β equal to 0.44‰ (or about 1/2286), which is more than 2 times lower than the one achieved by the uncoupled model (that is equal to 1.00‰). However, during the progressive application of the imposed settlement patterns for coupled models, the differences between the soil β and the interface β reduce, as the façade progressively gets damaged, and thus becomes more flexible and able to better accommodate the imposed settlement. The same observation can be made when looking at the trend of the interface β against the façade β, in this case for both coupled and uncoupled models (Fig. 4e, f). It can be then concluded that for coupled models, the imposed distortion gets significantly reduced at the interface level, whereas it only slightly decreases at the façade level; Conversely, for uncoupled models, the distortion at the top of the soil block is not significantly affected by the soil stratum, and it is almost equal to the one imposed at the bottom, whereas it gets flatten down when it reaches the bottom of the façade. Both

Input vs Output displacements for **Coupled** and **Uncoupled** models in **Hogging** for different **Soil heights** (in mm)
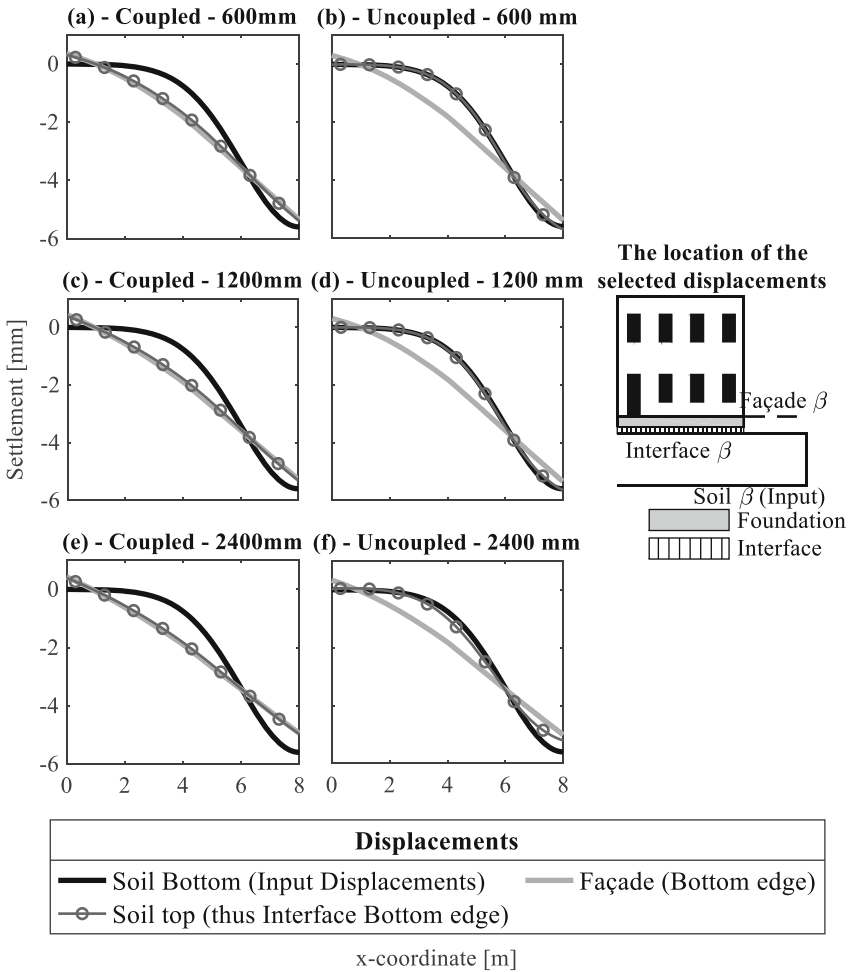
Fig. 4. Vertical displacements for coupled model and uncoupled model in *hogging* for an applied angular distortion equal to 1.00‰ (or 1/1000) at step 112 in hogging for a soil height of 600 mm for (a) and (b), 1200 mm for (c) and (d), 2400 mm for (e) and (f).

modelling approaches exhibit consistent trends of soil β against the façade β (Fig. 4c, d) for a given settlement pattern, for the soil height equal to 600 mm; This indicates that, although the displacements at the interface level differ, the adopted interface typologies, i.e., contact and boundary interfaces, do not significantly influence the ratio between the imposed soil deformation and the one retrieved along the façade for small soil heights.

Results for **Coupled** and **Uncoupled** models for different soil heights
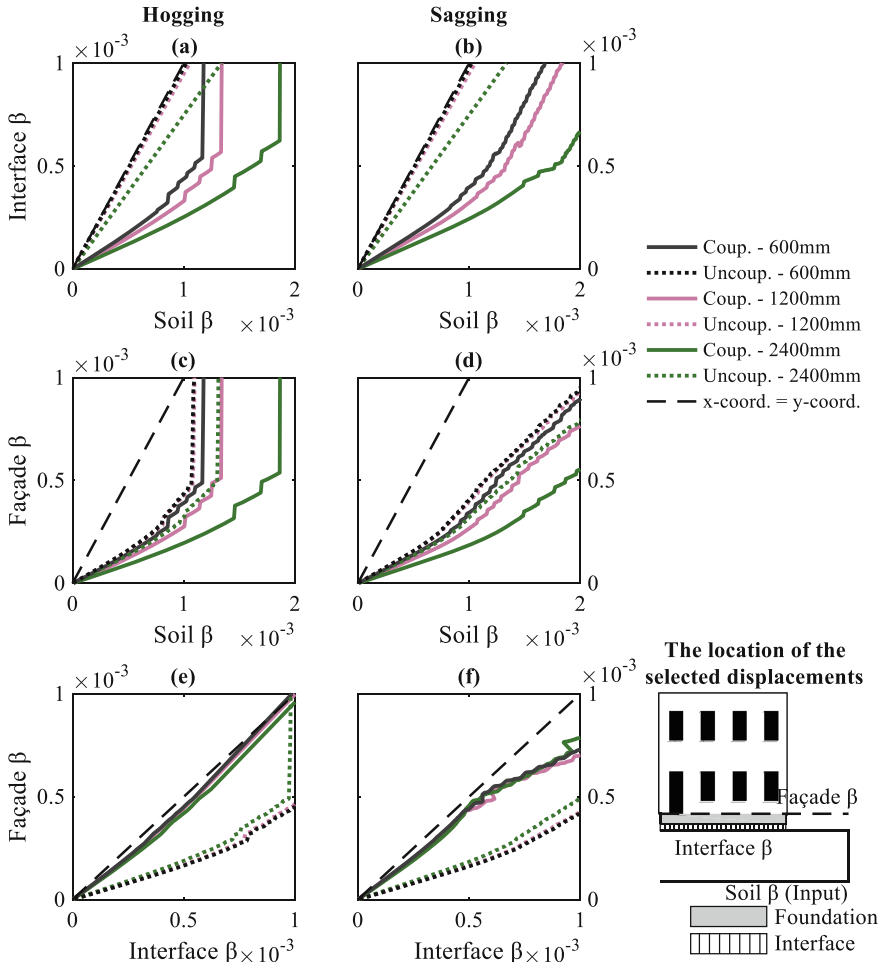
Fig. 5. Angular distortion values for coupled (Coup.) model and uncoupled (Uncoup.) model and sagging for different soil heights. The plots show the relative rotations computed from the input displacements and the displacements retrieved at the bottom of the interface and the bottom of the façade. The plots focus on the values of the angular distortions associated with light damage, i.e., Ψ lower than 3. The dashed line shows the trend for which the values of the x- and y-axis would be equal.

4.2 Interface Stresses

Figure 6 shows the vertical interface stresses in both hogging and sagging for both coupled and uncoupled models for an applied angular distortion equal to $1.00‰$ (or $1/1000$) for the soil height of 600 mm.

For the selected angular distortion, the models in sagging exhibit the formation of a gap in the middle of the façade as part of the interface reaches zero compressive stresses;

The formation of the gap is related to the use of no-tension interfaces, which avoid an unrealistic pulling of the façade due to the ground movements [4].

Conversely, in hogging the entire interface is compressed. Regarding the differences between the coupled and uncoupled models, both modelling approaches show similar vertical interface stress components underneath the foundations.

Coupled model - Hogging
Max: -1.35e-02 N/mm^2
Min: -6.45e-02 N/mm^2

Uncoupled model - Hogging
Max: -1.36e-02 N/mm^2
Min: -6.36e-02 N/mm^2

Coupled model - Sagging
Max: 0.00e+00 N/mm^2
Min: -5.31e-02 N/mm^2

Uncoupled model - Sagging
Max: 2.16e-04 N/mm^2
Min: -5.47e-02 N/mm^2

-0.06   -0.05   -0.04   -0.03   -0.02   -0.01   0
Normal Interface stresses at step 112 (Imposed Soil $\beta = 1/1000$) [N/mm^2]
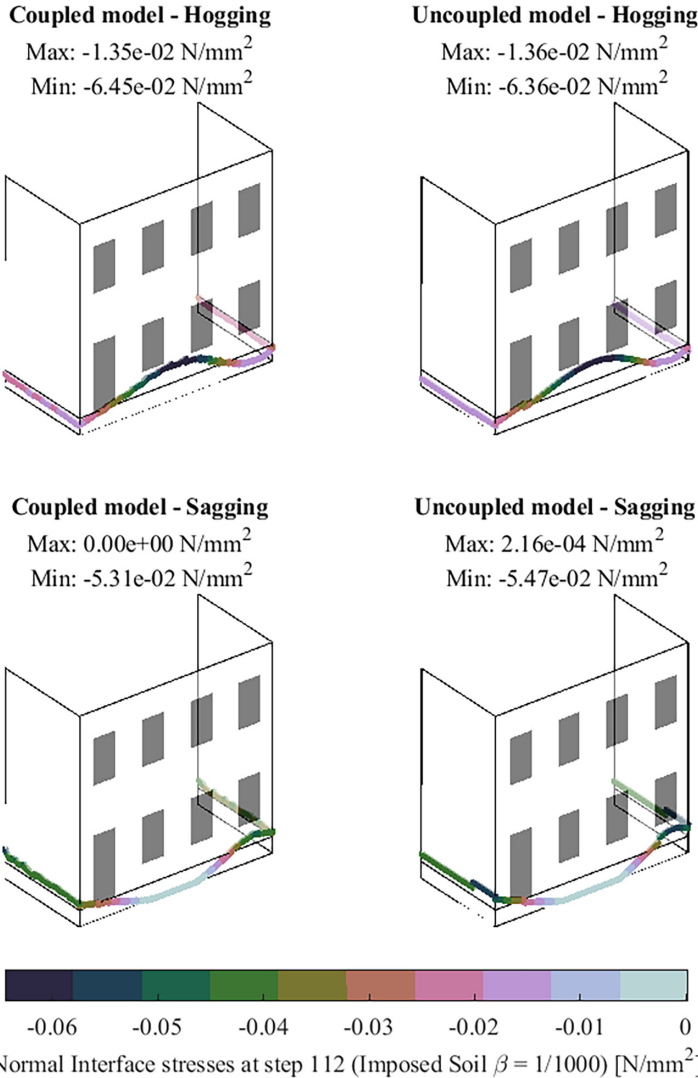
Fig. 6. Normal interface stresses for hogging and sagging, with applied angular distortion of 1.00‰ (or 1/1000) at step 112 of the settlement phase of the numerical analyses. Negative values represent compression.

4.3 Damage

Figure 7 shows the crack pattern obtained at different values of the imposed angular distortion for models coupled and uncoupled with the soil height equal to 600 mm subjected to hogging. Both the modelling approaches show similar crack patterns with cracks that initiate at the corner of the openings and propagate during the settlement application. Regarding the damage severity, the uncoupled model exhibits slightly higher Ψ values for the three selected steps.
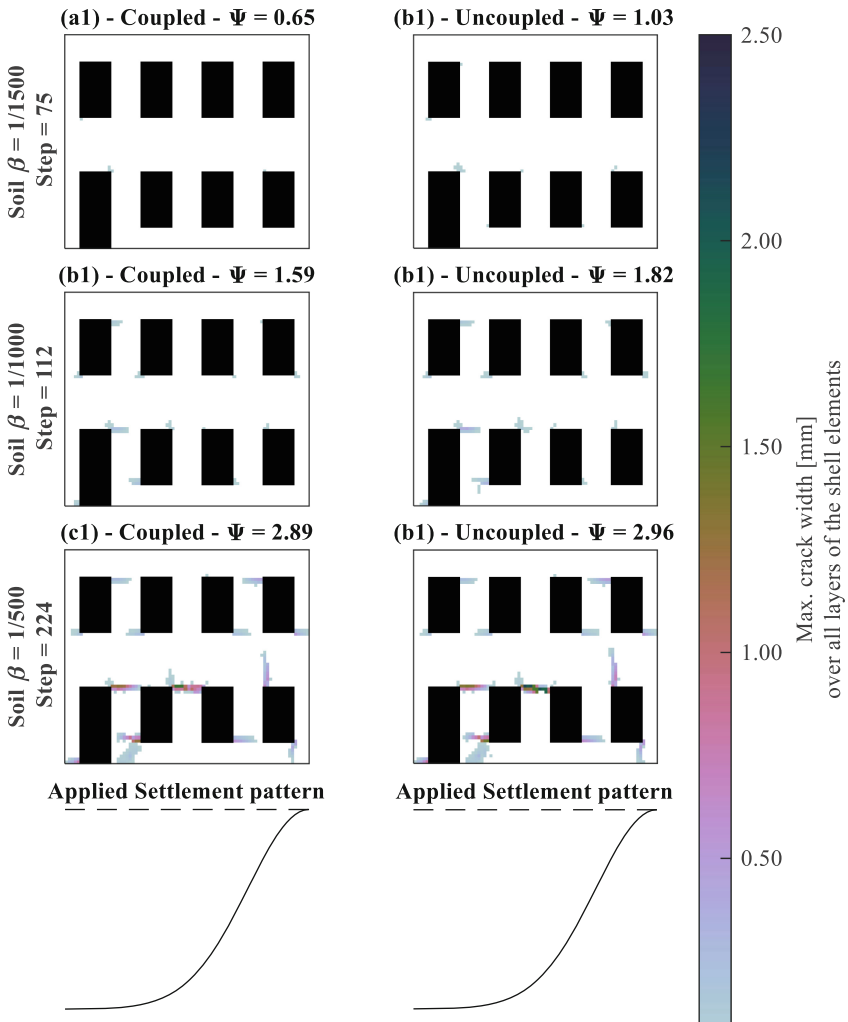

Fig. 7. Crack patterns in sagging for different steps of the analyses during the settlement phase for the models with a soil height of 600 mm.

The values of the imposed angular distortion, i.e., from the displacements imposed at the bottom of the soil block, and the angular distortion computed from the displacements at the façade level can be plotted against Ψ for all the steps of the numerical analysis. As this study focuses on the initiation and progression of the light damage, the plots focus on values of Ψ smaller than 3; Fig. 8 shows these trends for both hogging and sagging and all the selected soil heights, providing an overview of the results of all the models.
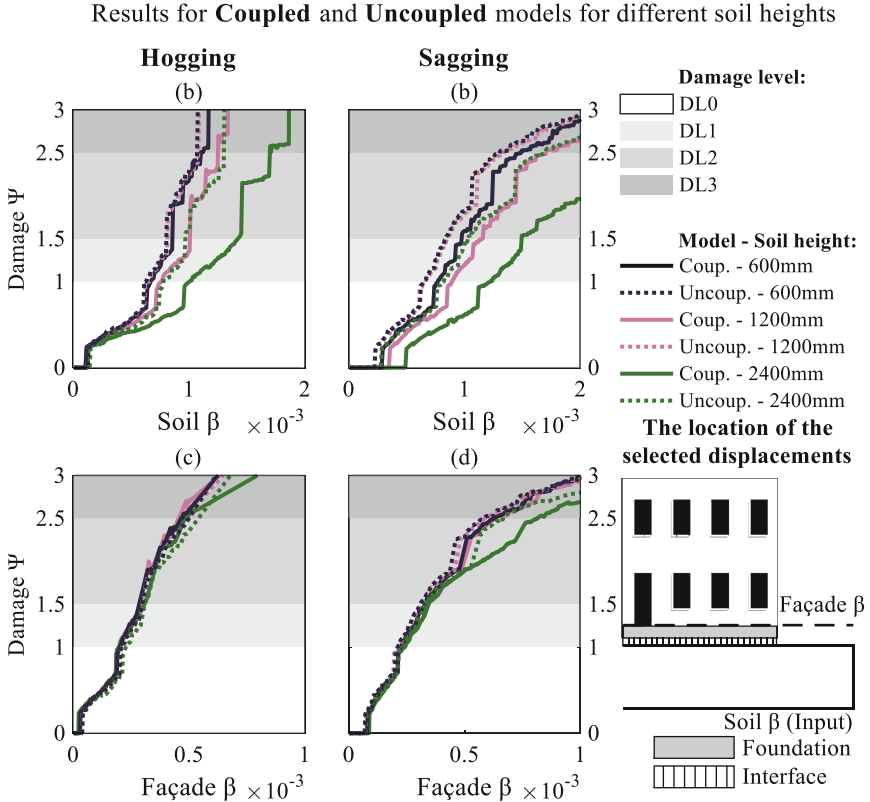

Fig. 8. Angular distortion against the resulting damage for all the coupled and uncoupled models for both hogging and sagging. The approximate crack width ranges corresponding to damage parameter Ψ (Table 3) are shown.

Figure 8a, b show that the models with the highest soil height, as expected, result in less damage for the same applied angular distortion at the soil bottom boundary, i.e., soil β, as the soil block with a height of 2400 mm was observed to decrease the imposed distortion (Fig. 4). Moreover, the good match between the results of the coupled and uncoupled models is observed with a soil height of 600 mm, in both hogging and sagging, with the uncoupled model resulting in Ψ values slightly higher than coupled for a given soil height, as also observed in Fig. 7.

Figure 8a show that the damage initiation in hogging is achieved for values of the soil angular distortion β equal to 0.12–0.15‰ (or about 1/9000) for both coupled and

uncoupled models. In sagging, however, Fig. 8b shows that the damage initiates first in uncoupled models for values of the soil β equal to 0.23–0.28‰, whereas coupled analyses exhibit damage starting from values of soil β ranging between 0.29–0.5‰.

Nevertheless, the plots in terms of façade β, i.e., the angular distortion β computed from the displacements at the façade base, and damage Ψ exhibit almost identical for all the models in both hogging (Fig. 8c) and sagging (Fig. 8d). This confirms that, for a given settlement shape, the distortion of façade associated with a certain damage severity does not depend on the type of modelling approach; Conversely, the modelling approach and the soil height influences the value of the imposed angular distortion required to reach a certain distortion in the façade. This is in agreement with the findings of previous studies, e.g., [5].

4.4   Analysis Time and Convergence

The analysis time and number of non-convergent steps of all the models are reported in Table 4. However, the analysis time is not considered to be an objective measure, as it could vary depending on the available computational resources. Therefore, Table 4 reports the normalized analysis time, arbitrarily considering as the reference cases the coupled models with a soil height equal to 600 mm. On average, all the coupled models show similar analysis time to their uncoupled counterparts. The number of non-convergent steps is also in hogging, better convergence is achieved in sagging by coupled models.

4.5   Mesh Size

The mesh size of the numerical models is a parameter that could strongly influence the results of the analyses. The numerical models herein presented adopt a mesh size of 200 × 200 mm, as briefly discussed in Sect. 3.1. Additional analyses evaluate the effect of different mesh sizes, i.e., 100 × 100 mm, and 50 × 50 mm for the coupled and uncoupled models with a soil height equal to 600 mm; The results are presented in Fig. 9.

Although the mesh size is not observed to significantly affect the results for models subjected to sagging (Fig. 9c, d), higher differences are observed in hogging for both coupled and uncoupled for Ψ values higher than 1.5. For both coupled and uncoupled models, the models with a mesh size of 100 × 100 mm and 50 × 50 mm show similar trends in hogging, suggesting that the mesh dependency can be reduced for smaller mesh sizes, although the analysis time increases significantly. For instance, the uncoupled model with a mesh size of 50 × 50mm subjected to hogging required about 100 times (i.e., 7–8 days) the analysis time of the same model with a mesh size of 200 × 200 mm (reported in Table 4). For all the models, the initiation of the damage, i.e. Ψ lower than 0.5, in both hogging and sagging is observed to not be influenced by the mesh size.

5   Discussion

In this research, a case study consisting of a masonry structure on a strip foundation is considered, which has already been used in previous studies [4–6]. The structural symmetry of the considered buildings is used to only model the façade and half portion

Table 4. A comparison of the performance of all the models in both hogging and sagging. The values of the coupled models with a soil height of 600 mm are shaded.

Model		Soil height [mm]	Analysis time [hh:mm:ss]	Normalized analysis time	Number of non-convergent steps
Hogging					
Coupled		600	02:22:24	1.00	36
Coupled		1200	03:15:58	1.38	38
Coupled		2400	03:05:17	1.30	21
Uncoupled	Soil	600	00:06:13	0.92	0
	Structure		02:05:15		20
Uncoupled	Soil	1200	00:12:08	1.13	0
	Structure		02:28:09		41
Uncoupled	Soil	2400	00:20:45	1.10	0
	Structure		02:16:06		49
Sagging					
Coupled		600	01:38:09	1.00	4
Coupled		1200	01:48:27	1.10	7
Coupled		2400	01:48:27	1.10	4
Uncoupled	Soil	600	00:06:12	1.16	0
	Structure		01:47:38		36
Uncoupled	Soil	1200	00:11:19	1.23	0
	Structure		01:49:40		38
Uncoupled	Soil	2400	00:19:28	1.15	0
	Structure		01:33:09		21

of each transverse wall. This is additionally made possible by the fact this work focuses on imposed settlement actions that do not present variations perpendicularly to the plane of the façade. The settlement shapes idealized hogging and sagging deformations due to the occurrence of subsidence processes in soil strata deeper than the one included in the models.

Two modelling approaches are selected from the state-of-the-art: a coupled model, in which a soil linear-elastic layer is modelled underneath the non-linear masonry structures, and an uncoupled model in which the soil volume is disconnected from the structure.

As the soil volume is elastic linear, it does not depict the response of the soil stratum, but it is used to aid the representation of the soil-structure interaction. The selected settlement actions are imposed at the base of the soil volume.

Different **mesh sizes** for **Coupled** and **Uncoupled** models
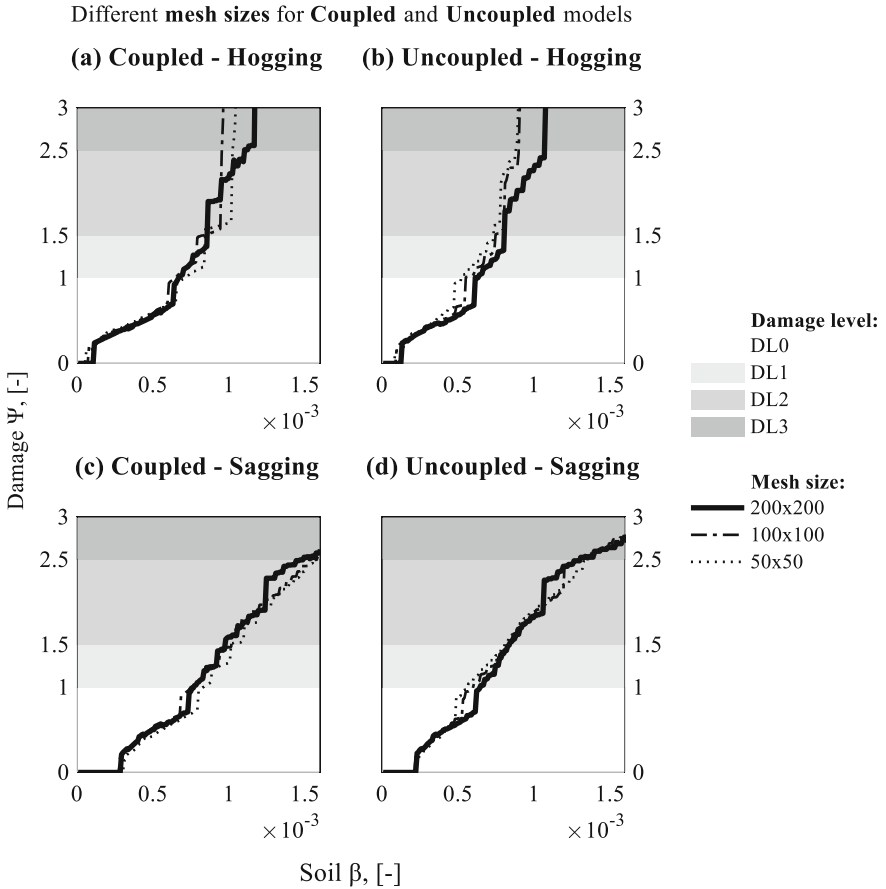
Fig. 9. Results of the numerical models in terms of imposed angular distortion against the resulting damage for selected mesh sizes in both hogging and sagging.

The soil-foundation interaction is herein simulated using two interface types, modelled beneath the masonry structure: contact interfaces for the coupled models, which link the soil volume and the structure and boundary interfaces for uncoupled analyses.

The adopted analytical formulation of the contact interfaces requires two soil parameters and the mesh size of the numerical model. The boundary interfaces use an analytical formulation that depends on two soil parameters and two additional geometric parameters, i.e., the foundation length and base.

The values of the vertical stiffness adopted for boundary interfaces, i.e., in uncoupled models, are one order of magnitude lower than the one adopted in the case of contact interfaces. The lower values are consistent with the fact that the boundary interface also represents the behaviour of the missing soil volume which is untied from the structural sub-system in the case of the uncoupled model.

The interface stresses present minor differences between coupled and uncoupled models and the response of the structure.

The influence of the soil volume is also investigated, by varying the parameter soil height, i.e., the depth of the soil represented in the models. Thus, the analyses are carried out by varying the height of the soil volume. As expected, increasing the soil volume decreases the magnitude of the distortion transmitted to the façade, flattening down the imposed deformation. Therefore, for a certain applied distortion, models with a higher soil height exhibit less damage. For instance, for an applied angular distortion equal to 1.00‰ (or 1/1000), the coupled model in hogging exhibits Ψ values equal to 2.2, 1.4, and 1.0 for soil heights equal to 600, 1200 and 2400 mm respectively. The most conservative prediction, i.e., the models with higher damage, is achieved with models that use the smallest soil height, both in sagging and hogging, and for both the modelling approaches.

The contribution of the soil sub-system in the case of the uncoupled models was observed to be negligible for a soil height equal to 600 mm. This supports the idea that the settlement pattern could be directly applied to the superstructure sub-system, in agreement with the methodology adopted by other studies, i.e., [3, 4, 6]. It is expected that soil heights higher than 600 mm should be used whenever the source of the settlement, i.e., the triggering phenomenon, is directly included in the model. The inclusion of a driver in the soil as a source of the deformation represents an additional level of complexity which is purposely neglected in this study. However, additional calibration and validation against a case study, in which detailed information is available, could further clarify the role of the investigated soil heights.

Regarding the adopted modelling strategies, a coupled model could be better suitable to model phenomena in which multiple parameters are applied at the same time in the models; for example, vertical displacements applied at the base of the soil volume and quantified by the angular distortion, and horizontal displacements, measured with horizontal strains applied to the soil volume.

The results prove that the uncoupled approach is more conservative, i.e., shows slightly more damage than the coupled model for the same imposed distortion.

Nevertheless, it is currently unknown whether the selected modelling strategies can accurately predict the response of existing structures, as validation data of real full structures, that includes information on the masonry material, the geometry of the building, the load distribution and the deformation pattern of both the soil and the structure are currently unavailable. It is however important to point out that similar modelling strategies were used in previous studies to reproduce with good agreement the behaviour of (parts of) existing structures or experimental benchmarks, e.g., in [30–32].

Finally, both modelling approaches show a similar convergence behaviour and computational time. Further analyses could investigate the effect of the settings of the numerical analyses on the results of the models, for instance changing the iterative method of the numerical solution, or the type of convergency norm and their tolerance.

6   Conclusions

In this study, two 3D modelling approaches selected from the state-of-the-art are used to investigate the behaviour of a masonry structure on a strip foundation subjected to settlements. The comparison between the selected modelling approaches is carried out

in terms of displacements, stresses and damage to the masonry façade. Thus, it was observed that:

- The crack pattern, i.e., the location and orientation of the cracks, during the application of the settlement, is observed to be consistent between the two modelling approaches.
- After the damage initiates, uncoupled models exhibit slightly more damage than the coupled models for a given value of imposed angular distortion, and are thus considered to be more conservative.
- Different displacements are observed beneath the interface of the coupled and uncoupled models: for coupled models, the imposed distortion gets significantly reduced at the interface level, whereas it only slightly decreases at the façade level; Conversely, for uncoupled models, the distortion at the top of the soil block is not significantly affected by the soil stratum, and it is equal to the one imposed at the bottom, whereas it gets flatten down when it reaches the bottom of the façade.
- Although the displacements at the interface level differ between the two modelling strategies, the adopted interface typologies, i.e., contact and boundary interfaces, do not influence the ratio between the imposed soil deformation and the one retrieved along the façade.
- Both interface typologies show similar values of vertical stresses along the interfaces beneath the foundations.
- For both modelling approaches, the damage to the façade depends on its deformation which, in turn, depends on the shape of the imposed settlements.
- The performance of the coupled and uncoupled models, in terms of computational time, convergency and mesh dependency, is similar.
- Although the coupled and uncoupled models have similar results and performance, the uncoupled model could be better suited to evaluate the response of structures subjected only to vertical displacements: Due to the limited contribution of the soil stratum for small soil heights in the case of uncoupled models, the superstructure sub-system can be used directly to evaluate the response of structures undergoing only vertical displacements, decreasing the modelling burden.

References

1. Deltares (2021) Technische toelichting risicokaarten funderingen
2. Erkens G, Kooi H, Melman R (2021) Actualisatie bodemdalingsvoorspellingskaarten. Deltares ed

3. Korswagen PA, Longo M, Prosperi A, Rots JG, Terwel KC (2023) Modelling of damage in historical masonry façades subjected to a combination of ground settlement and vibrations In: International conference on structural analysis of historical constructions. Springer, pp 904–917

4. Prosperi A, Longo M, Korswagen PA, Korff M, Rots JG (2023) Accurate and efficient 2D modelling of historical masonry buildings subjected to settlements in comparison to 3D approaches. In: International conference on structural analysis of historical constructions. Springer, pp 232–244

5. Prosperi A, Longo M, Korswagen PA, Korff M, Rots JG (2023) Sensitivity modelling with objective damage assessment of unreinforced masonry façades undergoing different subsidence settlement patterns. Eng Struct 286:116113

6. Prosperi A, Longo M, Korswagen PA, Korff M, Rots JG (2023) Shape matters: influence of varying settlement profiles due to multicausal subsidence when modelling damage in a masonry façade In: Tenth international symposium on land subsidence

7. Burd H, Houlsby G, Augarde C, Liu G (2000) Modelling tunnelling-induced settlement of masonry buildings. P I Civil Eng-Geotec 143:17–29

8. Burd H, Yiu W, Acikgoz S, Martin C (2022) Soil-foundation interaction model for the assessment of tunnelling-induced damage to masonry buildings. Tunn Undergr Sp Tech 119:104208

9. Giardina G, Rots J, Hendriks M. (2013) Modelling of settlement induced building damage

10. Netzel H, Kaalberg F. (2000) Numerical damage risk assessment studies on adjacent buildings in Amsterdam In: ISRM international symposium. ISRM-IS-2000-2596 ISRM

11. Son M, Cording EJ (2005) Estimation of building damage due to excavation-induced ground movements. J Geotech Geoenviron 131:162–177

12. Bowles J (1988) Foundation analysis and design. McGraw-Hill, Inc

13. Rots J, Messali F, Esposito R, Jafari S, Mariani V (2016) Thematic keynote computational modelling of masonry with a view to Groningen induced seismicity In: Structural analysis of historical constructions: anamnesis, diagnosis, therapy, controls: proceedings of the 10th international conference on structural analysis of historical constructions (SAHC, Leuven, Belgium, 13–15 September 2016). CRC Press, pp 227–238

14. Schreppers G, Garofano A, Messali F, Rots J (2016) DIANA validation report for masonry modelling. DIANA FEA report

15. Korswagen PA, Longo M, Meulman E, van Hoogdalem C (2017) Damage sensitivity of Groningen masonry structures–experimental and computational studies: stream 1

16. NPR9998:2020en (2021) Assessment of structural safety of buildings in case of erection, reconstruction and disapproval—induced earthquakes—basis of design, actions and resistances

17. Govindjee S, Kay GJ, Simo JC (1995) Anisotropic modelling and numerical simulation of brittle damage in concrete. Int J Numer Meth Eng 38:3611–3633

18. DIANA FEA bv (2023) Theory manual (DIANA 10.8). Thijsseweg 11, 2629 JA Delft, The Netherlands

19. NEHRP (2012) NIST GCR 12-917-21 Soil–structure interaction for building structures. National Institute of Standards and Technology, US Department of Commerce, Gaithersburg

20. Gazetas G (1991) Foundation vibrations. Springer, Foundation engineering handbook, pp 553–593

21. Mylonakis G, Nikolaou S, Gazetas G (2006) Footings under seismic loading: Analysis and design issues with emphasis on bridge foundations. Soil Dyn Earthq Eng 26:824–853

22. Ferlisi S, Nicodemo G, Peduto D, Negulescu C, Grandjean G (2020) Deterministic and probabilistic analyses of the 3D response of masonry buildings to imposed settlement troughs. Georisk 14:260–279

23. Charles JA, Skinner HD (2004) Settlement and tilt of low-rise buildings. P I Civil Eng-Geotec 157:65–75
24. De Vent IAE. (2011) Structural damage in masonry: Developing diagnostic decision support
25. Prosperi A, Korswagen PA, Korff M, Schipper R, Rots JG (2023) Empirical fragility and ROC curves for masonry buildings subjected to settlements. J Build Eng 106094
26. Korswagen PA, Longo M, Meulman E, Rots JG (2019) Crack initiation and propagation in unreinforced masonry specimens subjected to repeated in-plane loading during light damage. Bull Earthq Eng 17:4651–4687
27. Burland JB, Wroth C (1975) Settlement of buildings and associated damage
28. Burland JB, Broms BB, De Mello VF (1978) Behaviour of foundations and structures
29. Grünthal G (1998) European macroseismic scale. European Seismological Commission (ESC)
30. Bejarano-Urrego L, Verstrynge E, Drougkas A, Giardina G, Bassier M, Vergauwen M et al (2019) Numerical analysis of settlement-induced damage to a masonry church nave wall. Springer, Structural analysis of historical constructions, pp 853–861
31. Drougkas A, Verstrynge E, Szeker P, Heirman G, Bejarano-Urrego LE, Giardina G et al (2020) Numerical modeling of a church nave wall subjected to differential settlements: soil-structure interaction, time-dependence and sensitivity analysis. Int J Archit Herit 14:1221–1238
32. Giardina G, Van de Graaf AV, Hendriks MAN, Rots JG, Marini A (2013) Numerical analysis of a masonry facade subject to tunnelling-induced settlements. Eng Struct 54:234–247